Synthesis, Characterization, and Catalytic Activity of Sulfonated Carbon-Based Catalysts Derived From Rubber Tree Leaves and Pulp and Paper Mill Waste

J Janaun[1], **E Sinin, S F Hiew, A M T Kong, F A Lahin**
Catalysis, Reaction Engineering & Drying Technology Research Group (CREDYT),
Universiti Malaysia Sabah, Jalan UMS, 88400, Kota Kinabalu, Sabah, Malaysia

E-mail: [1]jidon@ums.edu.my

Abstract. Sulfonated carbon-based catalysts derived from rubber tree leaves, and pulp and paper mill waste were synthesized and characterized. Three types of catalyst synthesized were sulfonated rubber tree leaves (S-RTL), pyrolysed sludge char (P-SC) and sulfonated sludge char (S-SC). Sulfonated rubber tree leaves (S-RTL) and sulfonated sludge char (S-SC) were prepared through pyrolysis followed by functionalization via sulfonation process whereas, P-SC was only pyrolyzed without sulfonation. The characterization results indicated sulfonic acids, hydroxyl, and carboxyl moieties were detected in S-RTL and S-SC, but no sulfonic acid was detected in P-SC. Total acidity test showed S-RTL had the highest value followed by S-SC and P-SC. The thermal stability of S-RTL and S-SC were up to 230^{o}C as the loss was associated with the decomposition of sulfonic acid group, whereas, P-SC showed higher stability than the S-RTL and S-SC. Morphology analysis showed that S-RTL consisted of an amorphous carbon structure, and a crystalline structure for P-SC and S-SC. Furthermore, traces of metal components were also detected on all of the catalysts. The catalyst catalytic activity was tested through esterification of oleic acid with methanol. The results showed that the reaction using S-RTL catalyst produced the highest conversion (99.9%) followed by P-SC (88.4%) and lastly S-SC (82.7%). The synthesized catalysts showed high potential to be used in biodiesel production.

Introduction

Biodiesel or fatty acid methyl ester (FAME) that derived from vegetables oils or animal fats is a great alternative to fossil fuel. Due to the increasing price of petroleum and environmental concerns such as greenhouse effect and emission of particulate matter [1], alternative renewable fuels such as biodiesel have gained much attention.

In biodiesel synthesis, the reaction is facilitated with a suitable catalyst. Generally, the reaction on the production of biodiesel can be done with or without the presence of catalyst [2]. There are different types of catalyst that can be used in biodiesel production, which are homogeneous and

[1] To whom any correspondence should be addressed.

heterogeneous catalyst. Heterogeneous catalyst such as sulfonated carbon-based solid acid catalyst has recently reported as promising catalyst for biodiesel production [3].

Typically, base catalyst is more reactive than acid catalyst for biodiesel production. Nevertheless, base catalyst is suitable only for high quality feedstock (low FFA and water content) as opposed to acid catalyst where it can be used for low grade feedstock. This attributes promote the use of acid catalyst for large scale biodiesel production. It is more economical to produce biodiesel at a lower cost and this can be achieved by using low quality feedstock with higher catalytic activity. Low quality feedstocks which primarily contains high free fatty acids and water content, hence, producing a solid acid catalyst is ideal since it has the ability to carry out both the esterification of free fatty acid and transesterification of triglycerides simultaneously [2].

Solid acid catalyst, mainly sulfonated carbon-based catalyst can be prepared at a lower cost, environmental friendly and renewable therefore making catalysts such as sulfonated carbon-based catalyst, with a high conversion and low cost of production from renewable sources is needed for the production of biodiesel.

In this study, the readily available resources in large quantity, rubber tree leaves and pulp and paper mill waste, were utilized as the carbon precursors to synthesize sulfonated carbon-based catalysts. Their catalytic activity was tested on the esterification of oleic acid with methanol. The catalysts were characterized using modern analytical tools in order to understand their catalytic activity.

Preparation of Catalyst and Reactivity Test

1.1. Preparation of Carbon Supports

The samples were initially prepared according to an established method by [4] to prepare amorphous structured carbon support. All samples were pyrolysed in a Thermolyne 79300 Tube Furnace using Eurotherm 2116 Controller under 100 mL/min nitrogen atmosphere at 400^{o}C for 4 h. After that, the resultants were grounded and sieved.

1.2. Functionalization of Chars via Sulfonation

The carbon char was then functionalized by heating in fuming sulfuric acid (20 wt.% free SO_3; 40 mmol loading for 20.0 g of char) at 150^{o}C for 12 hours under nitrogen atmosphere at the flow rate of 100 mL/min. The resultants were then washed with hot distilled water until it reached constant pH, and there was no sulfate ion detected in the washed water. The samples were then dried at 100^{o}C overnight to remove moistures from the samples using Memmert Universal Oven Model 400. The samples were denoted as Sulfonated Rubber Tree Leaf (S-RTL), Sulfonated Suldge Char (S-SC) and Pyrolyzed Sludge Char (P-SC). P-SC sample had not undergone the functionalization process.

1.3. Catalysts Characterization

The catalyst samples were characterized for their chemical and physical properties. The catalyst total acidity was measured using acid (0.02M HCl)-base (0.01M NaOH) back-titration method. The functional groups of the char were determined by using Fourier Transform Infrared Spectrometry (FTIR). The catalyst was scanned at a range from 650 cm^{-1} to 4000cm^{-1} on Perkin Elmer spectrum 100. Energy-dispersive X-ray microanalysis (EDX) (Bruker Quantax Esprit 1.0) used to determine the composition of the features in the SEM image with the target composition configuration setting of Carbon, Sulphur, and Oxygen. The analysis molecular structure was determined using Philip Expert pro X-ray diffraction (XRD) (Philips Expert Pro pw3040) analysis using Cu-Kα radiation source scanned from angle 5 to 80 (2Θ). Besides that, Z-5000 Polarized Zeeman Atomic Absorbance Spectrophotometer (AAS) was used for the analysis of metal elements for the catalyst as there were five standard solutions selected metal elements prepared which includes calcium, potassium, magnesium, zinc and sodium. The porosimetry analysis were carried out using Automated Mercury Porosimeter by Thermo Pascal 440 Series as the samples tested from atmospheric to 200Mpa pressure

using medium gradual pressure increase and decrease. Determination of thermal stability was studied using Thermal Gravimetric Analysis (TGA) as each catalysts sample was analysed at a temperature rate of 10°C/min until it reached 400°C under nitrogen atmosphere.

1.4. Esterification Reaction of Oleic Acid with Methanol

In this study, oleic acid was used as FFA model feedstock for the reactivity test. The molar ratio of oleic acid to methanol used was 1:10 with catalyst loading of 0.3wt% with respect to the oleic acid, stirred at 800 rpm for 5 hours. The reaction temperature was conducted at 60°C. Samples were analysed using titration method based on its relation to acid value.

1.5. Acid Value

The concentration of the free fatty acid can be determined using titrimetric method by determining its corresponding acid value to the real concentration of oleic acid. In this study, 0.1M Potassium Hydroxide (KOH) was used as titrant while diethyl-ether and ethanol was used as the solvent with a mixture of diether-ether:ethanol (v:v) (1:1) using phenolphthalein as the end-point indicator. Result of titration is expressed in form of acid value. The equation of acid value is shown below:

$$\text{Acid Value} = (\text{A} - \text{B}) \times \frac{56.1\text{g}}{\text{mol}} \times \frac{\text{M}}{\text{m}} \quad (1)$$

(A-B) is the volume of the titrant used (ml), **M** is the concentration of KOH solution (mol/L) while **m** is the weight of sample (g). To calculate the conversion of oleic acid to biodiesel, the result can be further expressed in term of conversion percentage. The conversion equation used shown below:

$$\text{Conversion}\,(\%) = \frac{\text{Initial acid number} \times \text{Final acid number}}{\text{Initial acid number}} \times 100\% \quad (2)$$

Results and Discussion

1.6. Characterization of The Catalysts

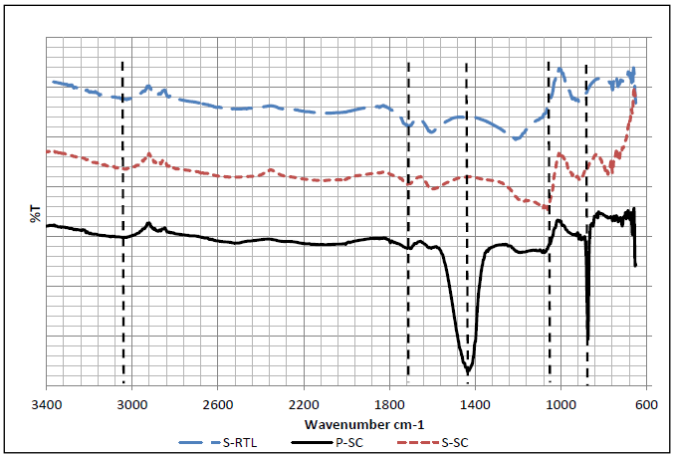

Figure 1. FTIR Spectra of S-RTL, P-SC and S-SC

Figure 1 shows the overall result of the FTIR for S- RTL, P-SC and S-SC. All samples showed bands at around ~1600 cm^{-1} which can be assigned to C=C stretching [5]. Moreover, a broad band was

observed in the region of 3400 cm^{-1} which were assigned to the –OH stretching modes of the –COOH and -OH groups. According to Méndez [6], the band between 3200 cm^{-1} to 3600 cm^{-1} could be attributed to the presence of hydroxyl groups of cellulose. This result suggested the presence of OH group in the catalyst. Besides that, the band at around ~1700 cm^{-1} in S-RTL and S-SC was assigned to the C=O starching mode of the COOH group [7], but it can be observed it is weak band at around ~1700 cm^{-1} for P-SC. Bands at 1010 cm^{-1} and 1004 cm^{-1} for S-RTL and S-SC can be attributed to the presence of S=O stretching [8]. Both samples showed bands at 1716 cm^{-1} attributed to the presence of SO_3H stretching. Therefore, FT-IR analysis showed that, there were SO_3H, -COOH, and –OH present in S-RTL and S-SC which was in agreement with literature [9] and [7]. However, SO_3H was not detected in P-SC only -COOH, and –OH moieties.

Table 1. Summary of Total Acidity of S-RTL, P-SC and S-SC

Catalyst	Total Acidity (mmol/g)
S-RTL	3.80 ± 0.05
P-SC	0.50 ± 0.02
S-SC	2.40 ± 0.04

Table 1 shows the summary of total acidity analysis by back-titration method. Based on the results in Table 1, S-RTL has the highest total acidity followed by S-SC, which is 3.80mmol/g and 2.40mmol/g, and P-SC with only 0.50mmol/g. According to Lee [10], it was mentioned that the higher value of total acidity than sulfonic group can be interpreted as due to the presence of many acid groups which include phenolic or carboxyl groups in addition to sulfonic groups in the catalysts. The high amount of total acidity in S-RTL is mainly related to the high amount of carbon content in the biomass.

On the other hand, the low amount of total acidity for P-SC can be related to the absence of sulfonic group. This was attributed to the presence of weak acid groups, which is –OH and –COOH, by the incomplete carbonization of pulp and paper mill waste (sludge). However, S-SC shows an increase in amount of total acidity after sulfonation suggesting that the presence of sulfonic group boosts the acidity of the sample.

Table 2. Average Concentration (ppm) of Metal Elements in Each Sample

Metal Elements	**Average Concentration (ppm)**		
	S-RTL	**P-SC**	**S-SC**
Ca	0.180	3.095	1.943
K	0.056	0.690	0.160
Na	0.243	6.672	1.475
Mg	0.013	0.909	0.000
Zn	0.005	0.000	0.015

Table 2 shows the average concentration of metal elements in each sample in terms of ppm analyzed using AAS. From the results, Ca, K and Na were detected in S-RTL, P-SC and S-SC. However, Mg was not detected in S-SC, which indicated by the negative value. Likewise, Zn was not detected in P-SC, but small concentration detected in S-RTL and S-SC. The composition of Ca in P-SC is higher compared to S-RTL and the amount decreases after sulfonation (S-SC). Metal species concentration reductions were obvious for Ca, K and Na. This probably due to the neutralization via sulfonation thus reduces the concentration of those particular elements.

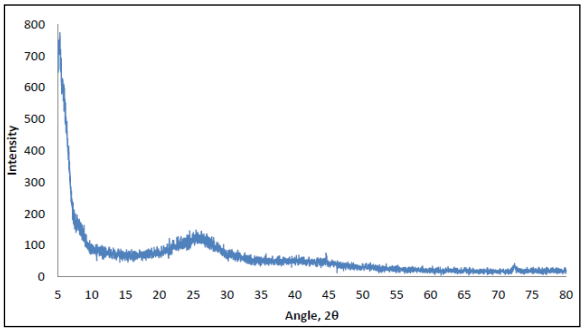

Figure 2. XRD Spectra of S-RTL

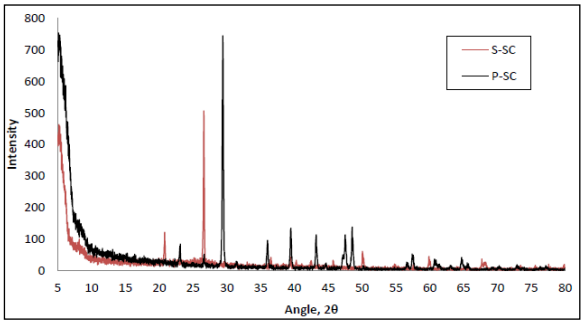

Figure 3. Superimposed XRD spectra of S-SC and P-SC

Figures 2 and 3 shows the results of X-Ray Diffraction plot analysis of S-RTL, and P-SC and S-SC, respectively. The analysis from XRD is important to determine the structure of carbon support as well as element identification. The XRD pattern exhibited diffraction peaks at 20 – 30^{o} (2θ) for sample S-RTL in Figure 2. This pattern is highly attributed to the non-graphitic carbon and indicated that this sample comprised of high non- graphitic carbon content [3]. Likewise, upon sulfonation this value is more consistent with the presence of amorphous carbon [11]. In addition, Mar et. al, [12] also recorded similar XRD pattern with the diffraction peaks which was assigned to amorphous carbon.

On the other hand, for both P-SC and S-SC show a strongest peak at 26.59^{o} and 29.39^{o} as seen in Figure 3 due to origination from the cellulose crystalline plane. The intensity of the peak for the bands of crystalline cellulose at this region after P-SC has been sulfonated (into S-SC) decreases as observed in Figure 3. This is probably due to its less cellulose content and the degradation took place after functionalization process [6]. Furthermore, P-SC shows peaks at 2 = 36.01^{o}, 39.40^{o}, 43.21^{o}, 47.49^{o} and 48.53^{o} which indicates that they were predominantly composed by calcite ($CaCO_3$) and small quantities of kaolinite as this data is in agreement with literature [6]. Likewise, the intensity of the peaks for P-SC at these regions decreases after sulfonation hence it can be inferred that the amount of $CaCO_3$ decrease after P-SC has been sulfonated (S-SC).

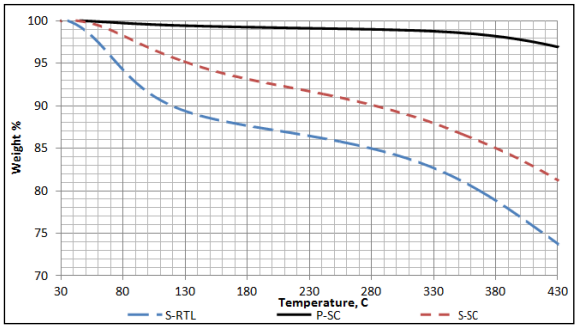

Figure 4. (a)

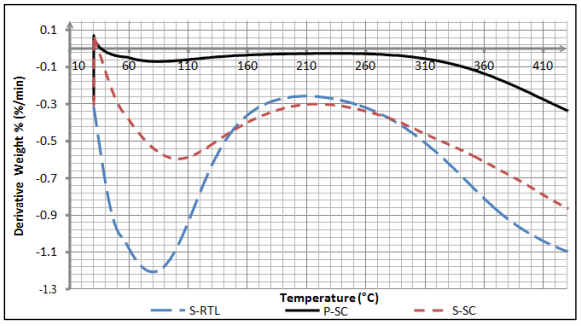

Figure 4. (b)

Figure 4. (a) Thermo-gravimetric Analysis (TGA) and (b) Derivative Thermal Analysis (DTA) of S-RTL, P-SC and S-SC under Nitrogen

Figures 4 (a) & (b) show the stability analysis graph derived on its TGA data. According to the results in Figure 4(a) it is clearly seen that, S-SC gradually starts to lose weight at 40^{o}C followed by S-SC at 50^{o}C and P-SC at 60^{o}C while in Figure 4 (b), the decrease in weight of all the samples at

around 90^{o}C can be attributed to the loss of moisture [4]. Furthermore, both of the S-RTL and S-SC recorded weak second stage weight loss around 230^{o}C though this trend was undetectable in sample P-SC. The second stage weight loss marks the first decomposition of the functional group on the surface of the carbon support interpreted as the loss of the sulfonic groups in agreement to literature [4] at that particular range of temperature. And so, it can be deduced that P-SC is more stable since the other samples starts to decompose important functional group faster.

Table 3. Porosimetry Data for S-RTL, P-SC and S-SC

Samples	S-RTL	P-SC	S-SC
Total Specific Surface Area	19.86	39.41	16.07
Total Porosity (%)	35.36	66.33	20.16
Average Pore Diameter (nm)	5104.42	2710.33	3375.53
Total Cumulative Volume (mm^3/g)	437.84	828.79	269.94

Table 3 shows the BET analysis using Automated Mercury Porosimetry in determining the total specific surface area and total porosity of S- RTL, P-SC and S-SC. P-SC sample shows the highest surface area followed by S-RTL and finally S-SC sample. The surface area of sample P-SC sample decreased after sulfonation (sample S-SC) and likewise, the same decrement trend was also recorded for the total porosity (%) of P-SC and S-SC sample as much as 46.17%. The reduction of pores and the surface area might be due to the penetration of acid groups into the surface of the porous pyrolysed sludge char, and the impregnation of -SO_3H groups into the pores of the char [13] caused the internal pores of sample P-SC to collapse [4]. On the other hand, S-RTL was observed to have highest average pore diameter, while P-SC sample had the smallest average pore diameter compared to all of the samples. Due to these reasons; high total porosity as well as smaller average pore diameter, caused the P-SC sample to have higher total specific surface area as well as high total cumulative volume in contrast to S-RTL and S-SC.

1.7. Catalytic Activity of The Catalysts

Biodiesels are mainly comprised of many Fatty Acid Methyl Esters (FAME) components such as Methyl Palmitate, Methyl Oleate, Methyl Myristate, and many more. These components can be derived from their respective triglycerides or fatty acids through transesterification or esterification process respectively. In this study, Oleic Acid was used as a model compound to represent the production of biodiesel through esterification reaction with methanol to produce methyl oleate (biodiesel) catalysed by S-RTL, P-SC and S-SC. Equation (3) below shows the chemical equation of esterification reaction by oleic acid with methanol in the presence of a catalyst to produce methyl oleate and water as adapted from [4]. From equation (3), it can be seen that the reaction pathways for esterification is reversible. To overcome and push the reaction to the desired product pathway, which is the right side, Le Chatelier principle was applied by increasing the molarity of methanol ten times of the oleic acid during the reactivity analysis.

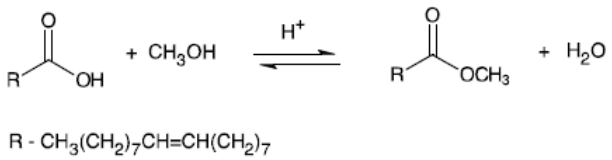

(3)

The esterification reaction of oleic acid with methanol requires 1 molar of oleic acid to produce 1 molar methyl oleate and hence through this information correlated with equation (1) and (2), the conversion of methyl oleate can be associated with the formation of oleic acid during the

reactivity test. Figure 5 shows the conversion percentage (%) of all the catalysts throughout the 5h reaction timespan. All of the conversions data were mathematically fitted using several mathematical models through computational means. The software used for the model fitting was OriginPro version 8.6. All of the lines were fitted with nonlinear curve fit method where S-RTL line was fitted growth/sigmoidal settings using Hill1 function model while samples P-SC and S-SC lines were fitted with exponential settings with ExpAssoc as its function.

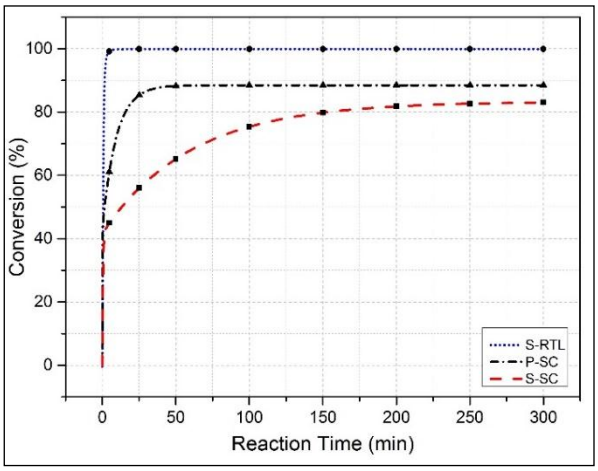

Figure 5. Graph of Conversion of Oleic Acid using S-RTL, P-SC and S-SC Catalysts

Table 4. Mathematical Fitting for Sample S-RTL, P-SC and S-SC

Catalyst	Mathematical Model Equation	Fitting (R^2)
S-RTL	$y = -0.46 + (100.36)\frac{x^{2.52}}{1.90 + x^{2.52}}$	0.999
P-SC	$y = -3.26\times10^{-17} + 45.83(1 - e^{-x/9.35}) + 42.63(1 - e^{-x/3.39\times10^{-4}})$	0.997
S-SC	$y = 5.31\times10^{-4} + 41.85(1 - e^{-x/0.51}) + 41.45(1 - e^{-x/0.56})$	0.990

Table 4 shows the mathematical fitting for sample S-RTL, P-SC and S-SC. The R^2 fitting value, which corresponds to the statistical measure of how close the data are to the fitted regression line, are all capped at 0.99 values thus displays high mathematical fitting for all the samples conversion lines.

By comparing all of these catalysts from the graph that was demonstrated in Figure 5, S-SC had the lowest formation rate compared to the others. All of the samples shows logarithmic conversion growth trend and reached maximum approximately at the 25th, 50th and 250th minutes of the reaction for catalyst S-RTL, P-SC and S-SC samples, respectively. The reactions were stopped after 5 hours. Among all of the catalysts, the reaction by using S-RTL contribute the highest conversion of oleic acid at the end of the reaction which are 99.86%, then P-SC (88.39 %) and lastly S-SC (82.65%).

S-RTL had the highest conversion may be associated to its highest total acidity among all other catalysts. The amorphous structure of S-RTL could have also contributed to the reactivity as amorphous structure is reported to be more flexible as opposed to the rigid structure of crystalline (P-SC and S-SC). Crystalline structure was arranged orderly compared to amorphous, hence it is very hard for the active site to attach into the catalyst. Similar result was reported by that of Toda et. Al [14].

In the FTIR analysis, the presence of sulfonic acid was detected in S-RTL and S-SC, however it was missing in P-SC. P-SC had the lowest total acidity compared to S-SC though it achieved higher conversion from the latter. This trend might be due to P-SC possessing higher total surface than S-SC.

In addition, the amount of metals on P-SC was higher than on S-SC. The presence of metal in the catalyst might have contributed to the higher catalytic reaction of P-SC.

Conclusions

Sulfonated carbon-based catalysts derived from rubber tree leaves, and pulp and paper mill waste were successfully synthesized, characterized, and tested its catalytic reactivity. Sulfonic acid moiety was detected in samples S-RTL and S-SC, whereas carboxyl and hydroxyl moieties were detected in all the samples including P-SC. The total acidity tests showed S-RTL had the highest total acidity of 3.80 mmol/g followed by S-SC (2.40 mmol/g) and P-SC (0.50 mmol/g). S-RTL and S-SC samples were thermally stable up to 230^{o}C, it was likely associated with the decomposition of sulfonic acid group. P-SC showed thermally more stable. XRD analysis suggested that S-RTL was an amorphous carbon structure, whereas P- SC and S-SC were a crystalline structure. Porosimetry analysis showed that P-SC had highest porosity of 66.33 %, followed by S-RTL (35.36 %) and S-SC (20.16 %), while the specific surface area of S-RTL, P-SC and S-SC were 19.86 m^2/g, 39.41 m^2/g and 16.07 m^2/g, respectively.

The conversion of oleic acid into methyl ester achieved more than 80% within 5 hours using all catalysts. In conclusion, S-RTL, P-SC, and S-SC are suitable catalysts for biodiesel production because they are highly reactive and thermally stable beyond the typical temperature of biodiesel reaction.

References

[1] Atadashi I M, Aroua M K, Abdul Aziz A R and Sulaiman N M N 2012 *Renew. Sustain. Energy Rev.* **16** pp 3456–3470
[2] Janaun J and Ellis N 2010 *Renew. Sustain. Energy Rev.* **14** pp 1312–1320
[3] Shu Q, Nawaz Z, Gao J, Liao Y, Zhang Q, Wang D and Wang J 2010 *Bioresour. Technol.* **101** pp 5374–5384
[4] Janaun J 2012 *Development of sulfonated carbon catalysts for integrated biodiesel production* Doctoral dissertation (Vancouver: The University of British Columbia)
[5] Jidon Janaun N E Preparation of Mesoporous Sugar Catalyst
[6] Méndez A, Fidalgo J M, Guerrero F and Gascó G 2009 *J. Anal. Appl. Pyrolysis* **86** pp 66–73
[7] Chen G and Fang B 2011 *Bioresour. Technol.* **102** pp 2635–2640
[8] Geng L, Wang Y, Yu G and Zhu Y 2011 *Catal. Commun.* **13** pp 26–30
[9] Janaun J and Ellis N 2011 *Appl. Catal. Gen.* **394** pp 25–31
[10] Lee D 2013 *Mol. Basel Switz.* **18** pp 8168–8180
[11] Deshmane C A, Wright M W, Lachgar A, Rohlfing M, Liu Z, Le J and Hanson B E 2013 *Bioresour. Technol.* **147** pp 597–604
[12] Mar W W and Somsook E 2012 *Procedia Eng.* **32** pp 212–218
[13] Pua F, Fang Z, Zakaria S, Guo F and Chia C 2011 *Biotechnol. Biofuels* **4** pp 56
[14] Toda M, Takagaki A, Okamura M, Kondo J N and al et 2005 *Nature* **438** pp 178